

## Docking Study of Bryostatins to Protein Kinase C $\delta$ Cys2 Domain

Kaname KIMURA,<sup>a</sup> Miho Y. MIZUTANI,<sup>a</sup> Nobuo TOMIOKA,<sup>a</sup> Yasuyuki ENDO,<sup>b</sup> Koichi SHUDO,<sup>b</sup> and Akiko ITAI<sup>\*a</sup>

*Institute of Medicinal Molecular Design, Key Molecular, Inc.,<sup>a</sup> 5–24–5 Hongo, Bunkyo-ku, Tokyo 113–0033, Japan and Graduate School of Pharmaceutical Sciences, The University of Tokyo,<sup>b</sup> 7–3–1 Hongo, Bunkyo-ku, Tokyo 113–0033, Japan. Received March 19, 1999; accepted May 24, 1999*

The docking structure of bryostatin 1, a potent activator of protein kinase C (PKC), to the crystal structure of PKC $\delta$  cys2 domain was examined computationally. Prior to the docking study, possible conformers of the 20-membered ring of bryostatin 1 were searched by the high-temperature molecular dynamics calculation method. For each conformer thus identified, the most stable docking model to PKC was searched without any presumptions, covering all possible binding modes and ligand conformations, using our automatic docking program ADAM. Among the seven conformers, the conformer with a ring conformation almost identical to that in the crystal (root mean square deviation=0.187 Å) yielded the most stable PKC–bryostatin 1 complex. The bryostatin molecule fits well to the cone-shaped bottom of the PKC binding cavity, forming four hydrogen bonds with main chain groups. On the basis of this docking structure, the structure–activity relations of various bryostatins are well explained.

**Key words** bryostatin 1; docking study; protein kinase C; structure–activity relation; conformation search; active conformation

Bryostatin 1 (**1a**) (Fig. 1), a macrocyclic lactone isolated from certain marine bryozoa such as *Bugula neritina* (Linnaeus), was discovered on the basis of its significant activity against murine P388 lymphocytic leukemia.<sup>1</sup> Many bryostatin congeners are known to be potent activators of protein kinase C (PKC),<sup>2</sup> which plays an important role in cellular signal transduction.<sup>3–5</sup> The molecules bind to the enzyme competitively with phorbol esters<sup>6–8</sup> such as 12-*O*-tetradecanoylphorbol-13-acetate (TPA, **2**), a tumor promoter, and diacylglycerol (**3**),<sup>9,10</sup> a lipid second messenger.<sup>3–5,11</sup>

In 1995, the crystal structure of PKC $\delta$  cys2 domain was elucidated in the complex with phorbol-13-acetate.<sup>12</sup> Although the domain is only a small part (50 residues) of the enzyme (674 residues), the phorbol-13-acetate molecule seems to be specifically recognized through four hydrogen bonds with main chain groups at the bottom of a binding cavity in this domain. As the phorbol-13-acetate OH group at C12 is located outside the cavity, as is the C13-acetate, in the complex, it was considered that a long fatty acid group at C12 or C13 might strengthen the binding to the domain by interacting with not only the surface of the domain, but also membrane constituents existing outside the cavity. Therefore, we were interested to know whether or not the activity of other known PKC ligands can be explained in terms of docking to this domain. In previous papers,<sup>13,14</sup> we have shown that teleocidins and their congeners can stably dock to the

domain, using our automatic docking program ADAM.<sup>15</sup> We have also confirmed that other well-known PKC ligands, aplysiatoxin and ingenol ester, can form complexes as stable as that of phorbol-13-acetate with the domain (unpublished data). We were next interested in examining the binding mode of bryostatins, which have extremely complex structures, by computational docking studies.

Here, we describe the results of a bryostatin ring conformer search by high-temperature molecular dynamics (HTMD) calculation, and docking studies of the conformers to the PKC $\delta$  cys2 domain. The structure–activity relations of various bryostatins are discussed based on the docking results.

**Ring Conformer Search of the 20-Membered Ring in Bryostatin 1** Prior to the docking study on bryostatins, possible conformers of the 20-membered ring in bryostatin 1 were searched. Although the crystal structure<sup>1</sup> of bryostatin 1 is consistent with the NMR-derived structure<sup>16</sup> of bryostatin 10 (Table 2), the possibility that some other ring conformer is the active one cannot be excluded. Conformational degrees of freedom inside the ring cannot be considered throughout the docking process by our automatic docking program ADAM.<sup>15</sup> So, in this study, possible ring conformers were searched by HTMD calculation, using a partial structure (**4**) as a model (Fig. 2).

The structure of **4** was prepared based on the crystal struc-

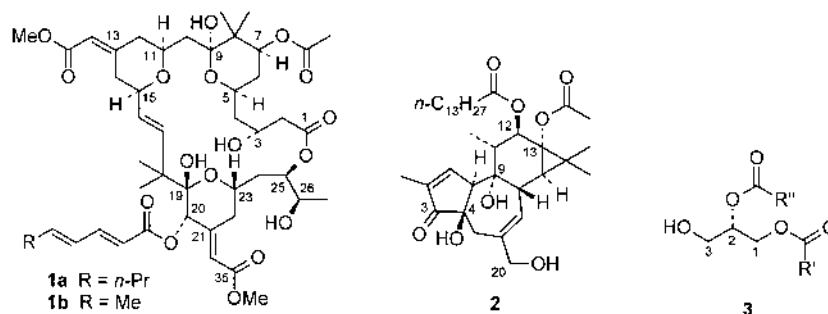


Fig. 1. Chemical Structures of PKC Activators

\* To whom correspondence should be addressed.

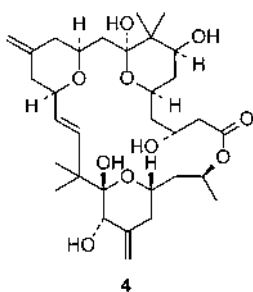


Fig. 2. Chemical Structure of 4

Table 1. Results of Conformer Search of 4 and Docking Simulation of 1b<sup>a)</sup>

	Conformer search of 4		Docking results of 1b			
	Energy	rms <sup>b)</sup>	$E_{\text{intra}}^{\text{c)}$	$E_{\text{inter}}^{\text{d)}$	$E_{\text{total}}^{\text{e)}$	H-Bond <sup>f)</sup>
Crystal	—	—	42.72	-38.82	3.90	4
Conformer 1	22.07	0.187	44.45	-36.94	7.51	4
Conformer 2	22.86	0.926	51.94	-33.00	18.94	3
Conformer 3	24.23	0.788	48.75	-30.95	17.80	3
Conformer 4	24.61	0.844	47.18	-31.87	15.31	4
Conformer 5	25.64	1.793	45.20	-18.83	26.37	1
Conformer 6	26.03	1.275	52.01	-35.04	16.97	4
Conformer 7	26.62	1.784	43.87	-22.78	21.09	1

a) Energies are in kcal/mol. b) rms: rms deviation from the crystal structure (Å). c)  $E_{\text{intra}}$ : intramolecular energy of the ligand. d)  $E_{\text{inter}}$ : intermolecular interaction energy between the protein and the ligand. e)  $E_{\text{total}}$ :  $E_{\text{intra}} + E_{\text{inter}}$ . f) H-Bond: the number of hydrogen bonds between the protein and the ligand.

ture<sup>1)</sup> of 1a taken from the Cambridge Structural Database (entry: BOKKIV), by removing substituent groups at C7, C13, C20, C21, and C26. All hydrogen atoms were relocated at appropriate positions. Atomic charges were calculated using the MNDO method in the MOPAC program.<sup>17)</sup> The HTMD calculation was performed at 1000K *in vacuo* using the AMBER program.<sup>18)</sup> Molecular dynamics trajectories were calculated with a time step of 0.001 ps. One thousand snapshot structures which were sampled during a 100 ps MD calculation were energy-minimized. Convergence criterion for norm of the gradient of the energy was 0.05 kcal/mol Å. These structures were superposed on each other by successive least-squares fittings and classified into typical conformers based on the root mean square (rms) deviation for 20 atoms constituting the 20-membered ring.<sup>19)</sup> By classifying structures with an rms deviation within 0.7 Å as a single conformer, seven conformers 1–7 with unique structures were obtained within 5 kcal/mol of the global energy minimum. These conformers were superposed onto the crystal structure to evaluate the resemblance. The intramolecular energies for the conformers and the rms values from the crystal structure are shown in Table 1. The structures are shown in Fig. 3. The global-minimum conformer (conformer 1) closely resembled the corresponding part of the crystal structure with an rms deviation of 0.187 Å.

**Computational Docking of Bryostatins to PKC** All docking studies on bryostatins to PKC were performed using the program ADAM which we developed.<sup>15)</sup> Stable docking models were automatically searched from all possible binding modes and ligand conformations. It is a characteristic of

our method that torsion angles in the ligand are repeatedly optimized in continuous conformation space during the docking process, affording accurate and reliable docking models.

The protein cavity was prepared from the crystal structure<sup>12)</sup> of PKC $\delta$  cys2 domain-phorbol-13-acetate complex taken from the Protein Data Bank (1PTR), by removing the phorbol-13-acetate molecule. As regards bryostatins to be docked, a model structure of bryostatin 1 (1b) was used to decrease conformational degrees of freedom. Deletion of the terminal two carbon atoms of the long substituent group at C20 in 1b seemed not to affect the docking result. Structures of 1b were modeled based on the crystal structure<sup>1)</sup> of bryostatin 1 and the seven ring conformers searched above with arbitrary torsion angles in rotatable bonds outside the 20-membered ring. Atomic charges in each conformer were calculated by the MNDO method in the MOPAC program.<sup>17)</sup> For each structure of 1b, docking study was performed independently and dozens of stable docking models were obtained from ADAM. To rank the docking models, the structures were optimized by the AMBER program,<sup>18)</sup> taking account of flexibilities in the protein structure. Then, the most stable docking model for each ring conformer was taken as a basis for discussion.

The docking results, *i.e.*, intramolecular and intermolecular interaction energies, the total (intra+inter) energy and the number of intermolecular hydrogen bonds, are summarized in Table 1 for the eight structures of 1b. The docking model for the crystal structure was most stable among them, both intramolecularly and intermolecularly. Among the seven conformers, conformer 1 gave the most stable docking model, which showed a close resemblance to that of the crystal structure, with the same hydrogen bonds (Fig. 4). In this model, the bryostatin molecule fits well into the cavity, with the C26 hydroxyl group at the pointed bottom of the cavity. The molecule forms four intermolecular hydrogen bonds with main chain groups: the C26-OH to both the NH of Thr242 and the carbonyl of Leu251, the C35-carbonyl to the NH of Gly253, and the C9-OH to the carbonyl of Met239. The hydrogen bond network is slightly different from that of the crystalline phorbol-13-acetate complex,<sup>12)</sup> in which the phorbol ester forms four hydrogen bonds as follows: the C20-OH to both the NH of Thr242 and the carbonyl of Leu251, the C3-carbonyl to the NH of Gly253, and the C4-OH to the carbonyl of Gly253.

The energy difference between the most stable model (conformer 1) and the second most stable one (conformer 4) was 7.8 kcal/mol (total energy). Although conformers 2, 3, 4, and 6 yielded stable docking models, they are less stable than that of conformer 1 because of insufficient contact with the surface of the cavity. Conformers 5 and 7 failed to form any stable complex, since they did not reach the bottom of the cavity.

**Structure-Activity Relations of Bryostatins** It was shown that bryostatin 1 can stably dock to the phorbol-13-acetate-binding cavity of the PKC domain in essentially the same conformation as that in the crystal structure of bryostatin 1. The docking model consistently explains the structure-activity relations<sup>11)</sup> of various bryostatins (Table 2). The fact that the binding affinities of bryostatins with various R<sub>1</sub> and R<sub>2</sub> groups (bryostatin 1 to 10, except for bryostatin 3

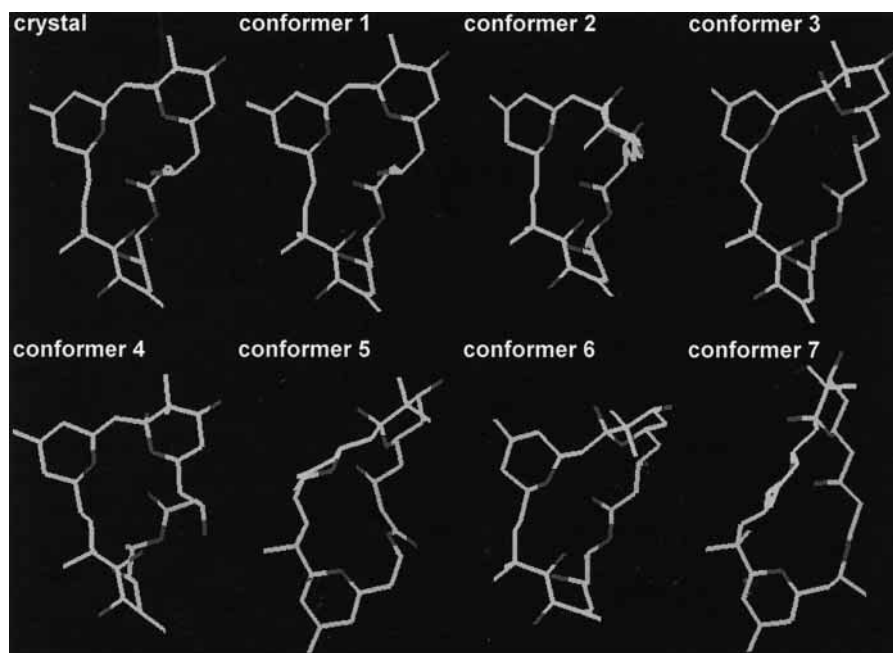


Fig. 3. Ring Conformations of **4** in the Crystal Structure and Seven Stable Conformers  
Hydrogen atoms are omitted for the sake of clarity.

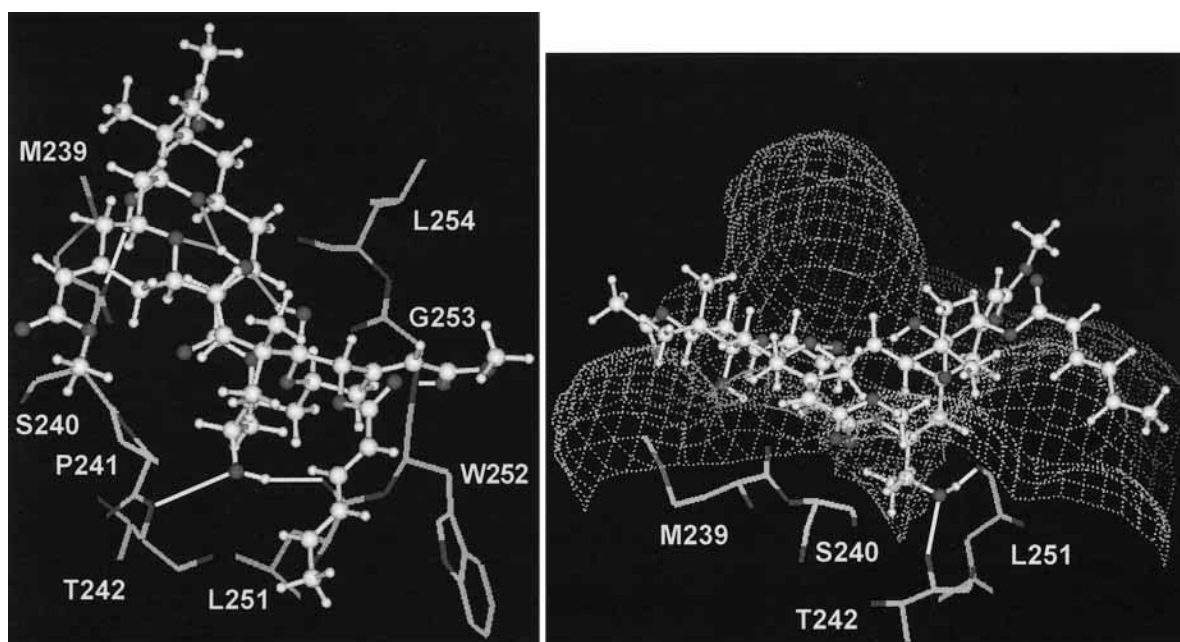


Fig. 4. The Most Stable Docking Model between PKC $\delta$  cys2 Domain and Bryostatin (**1b**: Conformer 1)

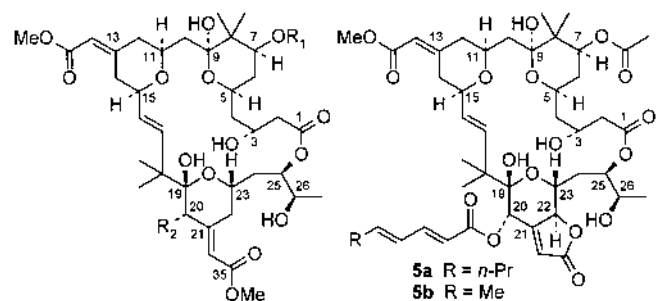
The bryostatin molecule is depicted in a ball-and-stick representation and the amino acid residues in the ligand-binding cavity of PKC $\delta$  cys2 domain are depicted in a wire-frame representation. Intermolecular and intramolecular hydrogen bonds are shown with yellow lines and cyan lines, respectively (distances less than 3.2 Å). (Left) A view of the ligand-binding cavity in the docking model to show the intermolecular interactions between the bryostatin molecule and various amino acid residues. (Right) Another view of the docking model to show the C26-OH group thrusting into the cone-shaped bottom of the ligand-binding cavity. The colored cage represents the surface of the allowed region for ligand and carbon atoms, calculated from the protein structure.

(**5a**) do not significantly differ from each other, is explained by the locations of the R<sub>1</sub> and R<sub>2</sub> groups in the docking model. Both groups are located outside the cavity, although the R<sub>1</sub> group fits into one of the two grooves on the surface of the domain. A separate docking computation using a model structure of bryostatin 3 (**5b**) which has a five-membered ring at C21 and C22, yielded an optimum docking structure almost identical with that of bryostatin 1. In the

model, a hydrogen bond is formed between the NH of Gly253 and the ester O of C22 instead of the carbonyl of C35 in **1b**.

The docking results imply that the C26-OH is essential for the activity. This is consistent with the fact that binding activity was lost in 26-acetylated bryostatin **4** and greatly reduced in 26-epi-bryostatin **1**. The 26-acetylation might cause severe steric hindrance at the bottom of the cavity, in addition

Table 2. Chemical Structures of Bryostatins and Binding Affinities to PKC

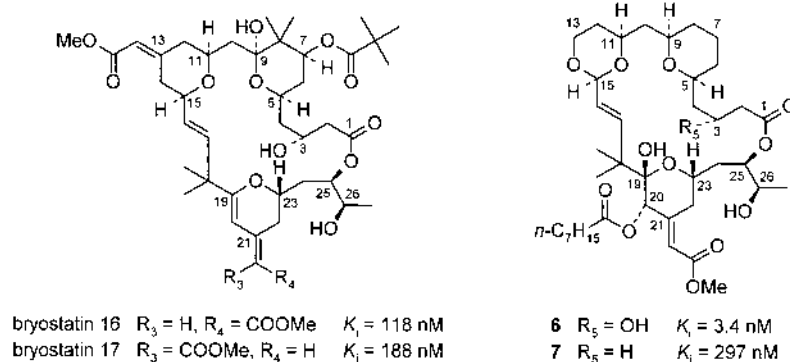


	R <sub>1</sub>	R <sub>2</sub>	K <sub>i</sub> (nM)
Bryostatin 1 (1a)	COMe	OOC-CH=CH-CH=CH- <i>n</i> -Pr	1.35
Bryostatin 2	H	OOC-CH=CH-CH=CH- <i>n</i> -Pr	5.86
Bryostatin 3 (5a)	H	OOC-CH=CH-CH=CH- <i>n</i> -Pr	2.75
Bryostatin 4	CO- <i>tert</i> -Bu	OOC- <i>n</i> -Pr	1.30
Bryostatin 5	CO- <i>tert</i> -Bu	OOCMe	1.04
Bryostatin 6	CO- <i>n</i> -Pr	OOCMe	1.18
Bryostatin 7	COMe	OOCMe	0.84
Bryostatin 8	CO- <i>n</i> -Pr	OOC- <i>n</i> -Pr	1.72
Bryostatin 9	COMe	OOC- <i>n</i> -Pr	1.31
Bryostatin 10	CO- <i>tert</i> -Bu	H	1.56
26-Acetylated bryostatin 4			>>100
26- <i>epi</i> -Bryostatin 1			32.6

These data were reported by Wender *et al.*<sup>11)</sup>

to loss of the hydrogen bonding partner. In 26-*epi*-bryostatin 1, the 26-methyl group might cause slight hindrance and unfavorable changes in surrounding atoms, from hydrophobic ones (the C $\beta$ , C $\gamma$ , C $\delta$  of Tyr238, the side chain of Leu251, and the C $\beta$ , C $\gamma$  of Gln257) to hydrophilic ones (the carbonyl of Tyr238, the NH and carbonyl of Ser240, the NH and OH of Thr242, and the amide of the side chain of Gln257), if the OH group forms hydrogen bonds in the same manner as in bryostatin 1.

The deletion of the C3-OH or C19-OH also reduces the binding affinity (Fig. 5).<sup>11)</sup> Both bryostatin 16 and 17, 19-*des*-OH analogues of bryostatin 1, show low affinities for PKC. Of the two synthetic analogues 6 and 7, 6 with the OH



bryostatin 16 R<sub>3</sub> = H, R<sub>4</sub> = COOMe K<sub>i</sub> = 118 nM  
 bryostatin 17 R<sub>3</sub> = COOMe, R<sub>4</sub> = H K<sub>i</sub> = 188 nM

6 R<sub>5</sub> = OH K<sub>i</sub> = 3.4 nM  
 7 R<sub>5</sub> = H K<sub>i</sub> = 297 nM

Fig. 5. Chemical Structures and PKC Binding Affinities of 19-*des*-OH Bryostatins and Synthetic Bryostatins (6, 7), Reported by Wender *et al.*<sup>11)</sup>

group at C3 shows almost the same activity as bryostatin 1, but 7 without the C3-OH group shows only weak activity (about 1%). With regard to the conformations of active bryostatins, bryostatin 10 and 6, structures with almost the same conformation as the crystal structure of bryostatin 1 were observed in solution.<sup>11)</sup> These results strongly suggest that both C3-OH and C19-OH are essential for the activity, playing a significant role in stabilizing the active conformation through intramolecular hydrogen bonds.

#### References and Notes

- Pettit G. R., Herald C. L., Doubek D. L., Herald D. L., Arnold E., Clardy J., *J. Am. Chem. Soc.*, **104**, 6846–6848 (1982).
- Nishizuka Y., *Nature* (London), **308**, 693–698 (1984).
- Berkow R. L., Kraft A. S., *Biochem. Biophys. Res. Commun.*, **131**, 1109–1116 (1985).
- Smith J. B., Smith L., Pettit G. R., *Biochem. Biophys. Res. Commun.*, **132**, 939–945 (1985).
- Kraft A. S., Smith J. B., Berkow R. L., *Proc. Natl. Acad. Sci. U.S.A.*, **83**, 1334–1338 (1986).
- Castagna M., Takai Y., Kaibuchi K., Sano K., Kikkawa U., Nishizuka Y., *J. Biol. Chem.*, **257**, 7847–7851 (1982).
- Driedger P. E., Blumberg P. M., *Proc. Natl. Acad. Sci. U.S.A.*, **77**, 567–571 (1980).
- Kikkawa U., Takai Y., Tanaka Y., Miyake R., Nishizuka Y., *J. Biol. Chem.*, **258**, 11442–11445 (1983).
- Takai Y., Kishimoto A., Kikkawa U., Mori T., Nishizuka Y., *Biochem. Biophys. Res. Commun.*, **91**, 1218–1224 (1979).
- Sharkey N. A., Leach K. L., Blumberg P. M., *Proc. Natl. Acad. Sci. U.S.A.*, **81**, 607–610 (1984).
- Wender P. A., DeBrabander J., Harran P. G., Jimenez J.-M., Koehler M. F. T., Lippa B., Park C.-M., Siedenbiedel C., Pettit G. R., *Proc. Natl. Acad. Sci. U.S.A.*, **95**, 6624–6629 (1998).
- Zhang G., Kazanietz M. G., Blumberg P. M., Hurley J. H., *Cell*, **81**, 917–924 (1995).
- Itai A., Matsuo A., Mizutani M. Y., Tomioka N., Shitaka M. T., Endo Y., Shudo K., *Chem. Pharm. Bull.*, **45**, 573–575 (1997).
- Endo Y., Takehana S., Ohno M., Driedger P. E., Stabel S., Mizutani M. Y., Tomioka N., Itai A., Shudo K., *J. Med. Chem.*, **41**, 1476–1496 (1998).
- Mizutani M. Y., Tomioka N., Itai A., *J. Mol. Biol.*, **243**, 310–326 (1994).
- Kamano Y., Zhang H.-P., Morita H., Itokawa H., Shirota O., Pettit G. R., Herald D. L., Herald C. L., *Tetrahedron*, **52**, 2369–2376 (1996).
- Stewart J. J. P., *J. Comput.-Aided Mol. Des.*, **4**, 1–105 (1990).
- Weiner P. K., Kollman P. A., *J. Comput. Chem.*, **2**, 287–303 (1981).
- Kawai T., Tomioka N., Ichinose T., Takeda M., Itai A., *Chem. Pharm. Bull.*, **42**, 1315–1321 (1994).